Dual-Mode Oscillator utilizing Higher Overtones of the SC-cut Resonator Operating over Extended Temperature Range

Vladimír Štofanik
Institute of Electronics and Photonics
FEI STU
Bratislava, Slovakia
vladimir.stofanik@stuba.sk

Peter Kubinec
Institute of Electronics and Photonics
FEI STU
Bratislava, Slovakia
peter.kubinec@stuba.sk

Elena Cocherová
Institute of Electronics and Photonics
FEI STU
Bratislava, Slovakia
elena.cocherova@stuba.sk

***Abstract*— This paper presents the dual-mode crystal oscillator (DMXO) that we designed, optimized, and evaluated over an extended temperature range from -45°C up to +215°C. The designed DMXO comprises two gain loops sharing a common 10-MHz 3rd-overtone stress compensated (SC) quartz resonator. The first loop ensures an excitation of the main 3rd overtone slow thickness-shear mode (i.e., the c mode), while the second loop ensures an excitation of the higher 5th overtone fast thickness-shear mode (i.e., the b mode) in the common volume of the SC resonator. One important advantage of this configuration is that the resonant frequency of the excited b mode is far from (approximately 82% above) the resonant frequency of the main excited c mode; hence the mode separation in the DMXO is simpler.**

Keywords*— *dual-mode oscillator, SC-cut, thickness-shear modes, quartz resonator, elevated temperatures

I. Introduction

Demand for reliable and robust dual-mode oscillators for harsh high-temperature and often high-pressure environment has been growing recently. Besides of frequency control applications, the robust oscillator circuits are required for driving novel dual-mode pressure / temperature piezoelectric sensors for down-hole explorations in the oil & gas industry; and they may be essential for future deep geothermal drilling technologies as well [1-3].

To implement the self-thermometry of the piezoelectric resonators at elevated temperatures, we need to design reliable dual-mode crystal oscillator (DMXO) circuits capable of operation at elevated temperatures as well. One example of high-temperature DMXO based on the two modified Butler oscillators forming two independent gain loops and sharing common stress compensated (SC) quartz resonator we described in [4]. In this case, the two slow thickness-shear modes, which are both stress and temperature-transient compensated, were utilized in the DMXO. The dual gain-loop DMXO can also incorporate properly designed mode-separation impedance filters to increase the isolation of the two gain loops from each other. To simplify the design of such filters, we derived the required formulas in closed analytical form [5]. This paper introduces the high-temperature (HT) DMXO we designed and evaluated over an extended temperature range between -45°C and +215°C. The DMXO comprises two gain loops. In the common volume of the used SC resonator, the first loop ensures an excitation of the 3rd overtone slow thickness-shear mode that is both temperature- and stress-compensated [6-7]; while the second loop ensures an excitation of the higher 5th overtone fast thickness-shear mode for which the resonant frequency almost linearly decreasing with temperature; hence this mode is well suited for the SC resonator's self-thermometry implementation.

This research was supported by the Ministry of Education of Slovak Republic under the grant VEGA No. 1/0711/23.

II. The Dual-Mode Crystal Oscillator Structure

A simplified schematic diagram of the DMXO, which we designed and optimized for operation at elevated temperatures and over a wide temperature range, is shown in Fig. 1. The DMXO consists of two modified Butler oscillators that share a common SC resonator. In this configuration, one terminal of the resonator is grounded. Reducing the emitter current of the bipolar junction transistor (BJT) provides negative feedback so that the feedback sufficiently reduces the net gain of the loop below unity for all frequencies except the frequency of the selected mode of vibration used in the respective gain loop. The two separation filters shown in Fig. 1 are connected between the non-grounded terminal of the SC resonator and the emitter of the corresponding BJT Q1 and Q2, respectively.

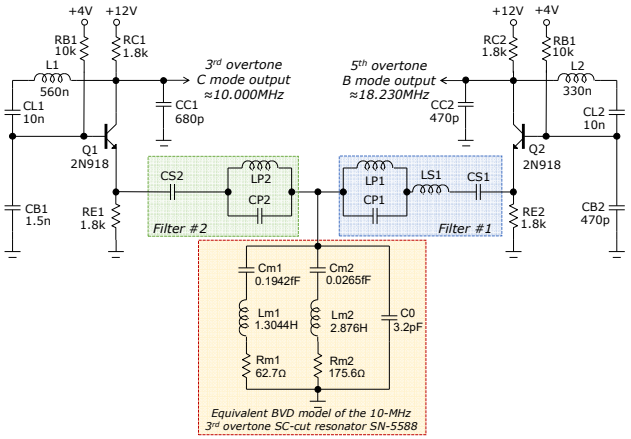

Fig. 1. Simplified structure of the HT DMXO with SC quartz resonator and the two mode-separation filters.

III. Mode-Separation Impedance Filters

The SC resonator, we utilize in the HT DMXO, simultaneously vibrates at the 3rd overtone c mode with approximately 10 MHz resonant frequency, and at the 5th overtone b mode with approximately 18.23 MHz resonant frequency. Hence, the two mode-separation impedance filters must be designed regarding these two resonant frequencies.

The mode-separation filter is the two terminal circuit forming required frequency dependent impedance. The filter must provide high impedance at the frequency which we want to isolate from the respective gain loop, and at the same time it must ensure the low impedance and ideally zero phase-shift at the frequency of the active mode in the corresponding gain loop of the DMXO. Since the emitter ac current of the active oscillator should flow through the SC resonator to the ground, it should also flow as a whole through the filter. Hence only two-pole filter structure shown in Fig. 2, without any branch to the ground, fulfills this requirement.

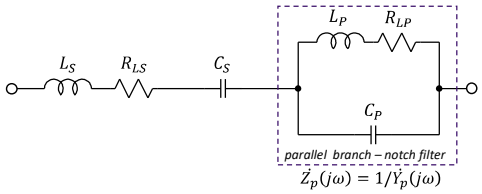

Fig. 2. Equivalent electric circuit of the mode-separation filter structure.

Impedance of the filter shown in Fig. 2 as a function of an angular frequency ω is:

$$\dot{Z}(j\omega) = R_{LS} + j\left(\omega L_S - \frac{1}{\omega C_S}\right) + \frac{1}{j\omega C_P + \frac{1}{R_{LP}+j\omega L_P}} \quad (1)$$

The parallel branch of circuit shown in Fig. 2 provides notch filter, with a maximum value of the impedance modulus at parallel resonant angular frequency:

$$\omega_{rp} = \frac{1}{\sqrt{L_P C_p}} \quad (2)$$

The first step of the mode-separation filter design is selection of the two components C_P a L_P for the notch filter (the parallel branch) according to the resonant frequency (2). The practical selection depends on other criteria such as adequate attenuation required for the defined loading impedance, and reliability and stability of component parameters over required operating temperature range as well.

The second step of the design of the mode-separation filter is the definition of the angular frequency ω_r at which the phase-shift of the filter impedance (1) needs to be zero; and at the same time the impedance modulus needs to be the very low. This condition will be fulfilled at the frequency, where the imaginary part of the complex impedance is equal to zero. Since the two gain loops of DMXO require the separation of the two modes of vibration excited in the common resonator from each other, the two separation filters must have these resonant angular frequencies interchanged:

$$\omega_{rp1} = \omega_{r2} = 2\pi f_{r2} \ , \ \omega_{rp2} = \omega_{r1} = 2\pi f_{r1} \quad (3)$$

In our case, for the used SC quartz resonator, the two resonant frequencies are: $f_{r2} \cong 10$ MHz and $f_{r1} \cong 18{,}23$ MHz.

The schematic diagram of circuit including designed separation filters and used for SPICE simulations of transfer frequency characteristics is shown in Fig. 3. The values of the R_{Lp1}, R_{Lp2}, and R_{Ls1} represent measured equivalent series loss ac resistances of the three corresponding air-core wire-wounded inductors at given resonant frequencies and the room temperature. Simulated transfer characteristics of both filters are shown in Fig. 4. Used real components are listed in Tab. 1.

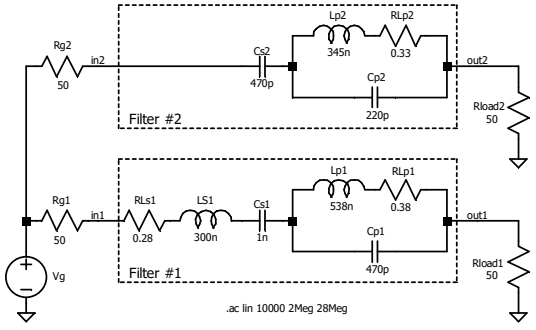

Fig. 3. Schematic diagram of the circuit used for SPICE simulations. The 50 Ω loading impedances were used in order to compare simulations with real measurements using the vector network analyzer with the 50 Ω system impedance.

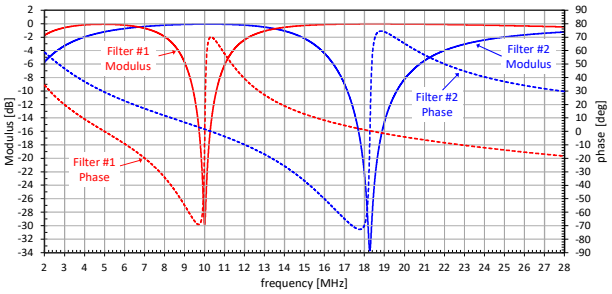

Fig. 4. Transfer frequency characteristics of the filters obtained from SPICE simulations (ac analysis); the loading impedances were 50 Ω.

TABLE I. COMPONENTS OF THE MODE-SEPARATION FILTERS

Filter #	L_P	C_P	L_S	C_S	*Band-stop IL @25°C*
#1	538nH 20T, Φ5mm AWG20	470pF COG 1206	300nH 11T, Φ5mm AWG20	1.0nF COG 1206	29.8dB
#2	345nH 12T, Φ5mm AWG20	220pF COG 1206	not used (short)	470pF COG 1206	33.6dB

IV. CHARACTERISTICS OF THE UTILIZED THICKNESS-SHEAR MODES OF THE SC-CUT QUARTZ RESONATOR

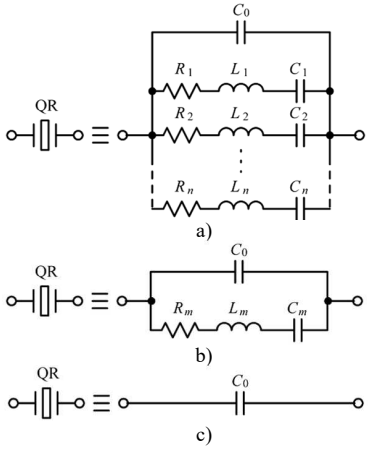

Fig. 5. Butterworth - Van Dyke equivalent linear model of the quartz resonator: a) in whole (or wide) frequency range; b) near to the selected "m" mode; c) in frequency range far away any mode of vibration.

Let us consider the Butterworth - Van Dyke (BVD) equivalent model of a quartz resonator (QR) shown in Fig. 5. In the frequency range, near the "m" mode it can be calculated impedance and admittance as follows

$$Z_{QR}(j\omega) = \frac{\left(R_m + j\omega L_m + \frac{1}{j\omega C_m}\right)\cdot\frac{1}{j\omega C_0}}{R_m + j\omega L_m + \frac{1}{j\omega C_m} + \frac{1}{j\omega C_0}} \quad (4)$$

$$Y_{QR}(j\omega) = \frac{R_m + j\omega L_m + \frac{1}{j\omega C_m} + \frac{1}{j\omega C_0}}{\left(R_m + j\omega L_m + \frac{1}{j\omega C_m}\right)\cdot\frac{1}{j\omega C_0}} \quad (5)$$

To determine the equivalent static capacitance C_0, as well as values of motional elements R_m, L_m and C_m representing the two respective thickness-shear in the SC resonator in the BVD model, we utilized technique based on measurements of complex scattering S_{11} vs. frequency characteristics measured by vector network analyzer. The steps and algorithms necessary for deriving the parameters utilize the scripts created in MATLAB we developed earlier [8-9]. The optimum fit of element values in the BVD equivalent model of the resonator (for appropriate mode), for which the minimum value of the error is reached, is based on the least squares method [8-9].

The results in the case of the slow 3rd overtone thickness-shear mode are shown in Fig.7; and in the case of the fast 5th overtone thickness-shear mode results are shown in Fig. 8. Derived values of equivalent elements for the BVD model of the used SC resonator are shown in Fig 1.

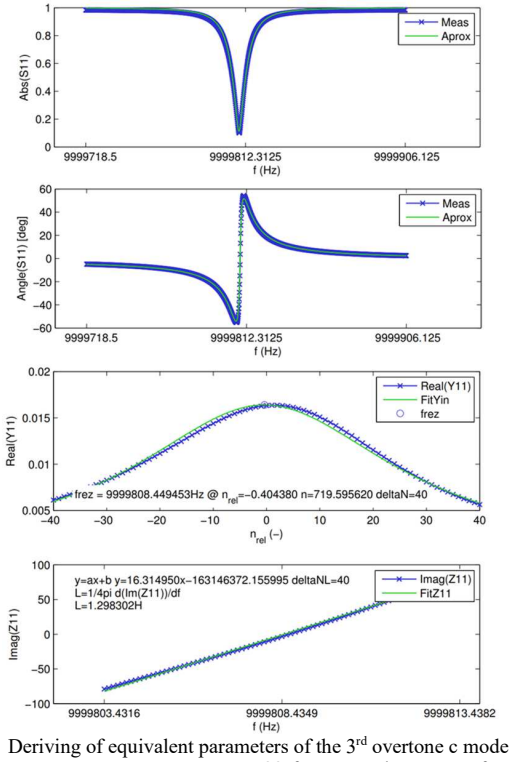

Fig. 6. Deriving of equivalent parameters of the 3rd overtone c mode of the utilized SC-cut quartz resonator SN5588 from complex S_{11} vs. frequency responses measured at the room temperature 25°C.

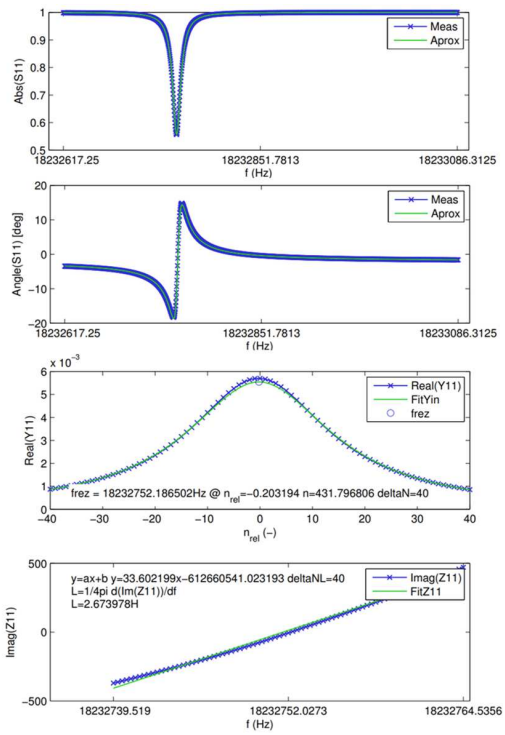

Fig. 7. Deriving of equivalent parameters of the 5th overtone b mode of the utilized SC-cut quartz resonator SN5588 from complex S_{11} vs. frequency responses measured at the room temperature 25°C.

V. Simulations of the Dual-Mode Crystal Oscillator

Schematic diagram of developed HT DMXO with SC quartz resonator and with the two separation filters is shown in Fig. 1. Note that the series ac resistances representing losses in the real inductors are not shown Fig. 1. However, the ac resistances of the inductors were considered within the SPICE simulations (transient analysis) as well.

The simulated waveforms of the Q1 and Q2 collector voltages and of the current through the resonator at the low temperature (-45°C), at the room temperature (25°C) and at the elevated temperature (+215°C) are compared in Fig. 8.

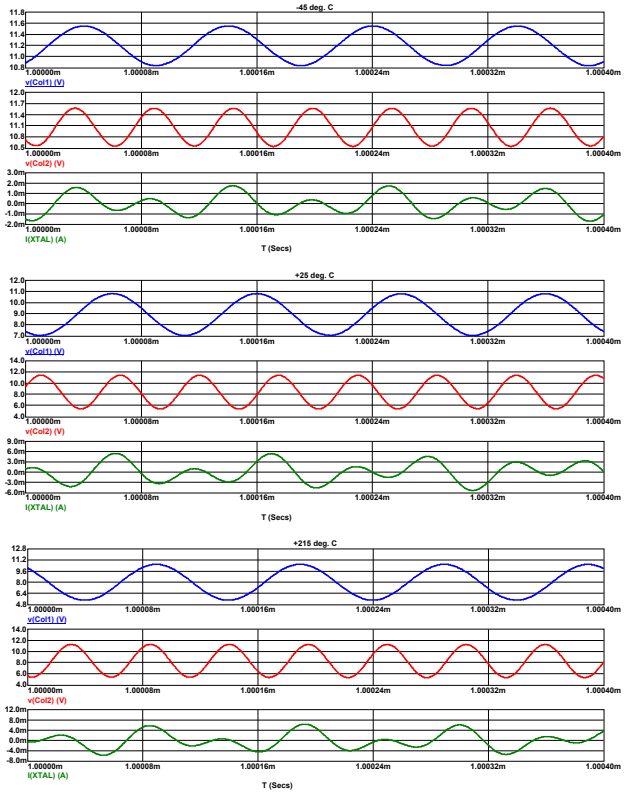

Fig. 8. Results obtained from the SPICE transient analyzis of the HT DMXO shown in the Fig 1. The waveforms of the Q1 colector voltage (blue), of the Q2 colector volatge (red) and of the current (green) flowing through the common SC resonator are compared at three temperatures: -45°C, +25°C and +215°C.

VI. Experimental Evaluation of the High Temperature DMXO Prototype

All electronic components used for the HT DMXO needs to reliably operate at elevated temperatures. The printed circuit board (PCB) and used solder need to withstand the elevated temperatures as well. We utilized high-temperature polyimide laminates, with the glass transition temperature at 250°C, for double-layer PCBs with galvanically gold-plated copper traces and pads. The used tin lead-free solder has a melting point at 230°C.

The SC quartz resonators are packaged in the cold-welded HC-40/U holders with gold plated terminals. The silicon military grade BJTs (2N918) are classified for long-term operation at 200°C. High-temperature thick multilayer resistors and class 1 ceramic COG (NPO) capacitors were used. The air-core inductors were in forms of single layer solenoids manually wounded from solid copper AWG-20 wire coated with polyimide enamel.

The inductors L1, L2, LP1, LS1 and LP2 shown in Fig. 1 should have the following number of turns: 21, 11, 20, 11 and 12, respectively. The internal diameter of all the solenoids is 5 mm. The two oscillators, as well as the two mode-separation filters were tuned to required resonant frequencies by manual stretching or compressing of turns of the corresponding solenoids at room temperature before the initial temperature-run in the temperature chamber.

Figure 9 illustrates the measured relative frequency vs. temperature variations of the two thickness-shear modes of the used SC quartz resonator simultaneously excited in the HT DMXO operating over the temperature range between -45°C and +215°C. Note that the two graphs represent the same characteristics, but in the two different scales to better compare the two excited modes of the SC resonator used.

Evaluation of continuous frequency vs. temperature measurements of the HT DMXO prototype recorded during several temperature runs in the chamber over the full range between -45°C and 215°C validated that both excited modes can operate reliably without any evidence of activity dips.

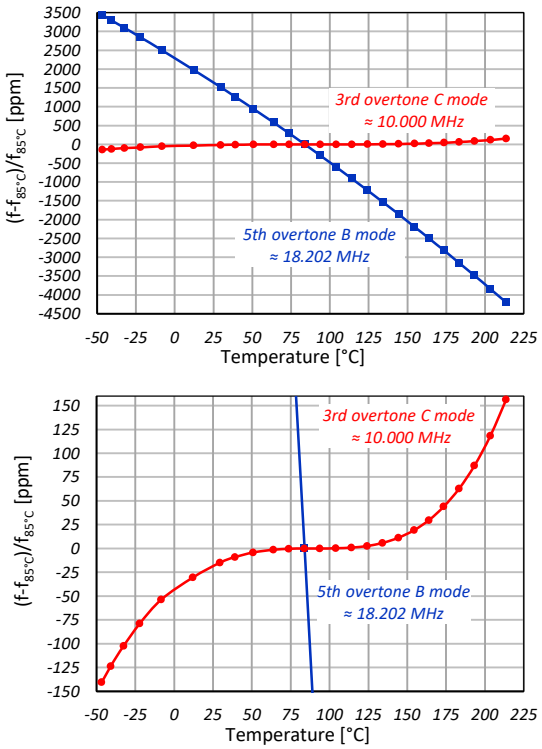

Fig. 9. Measured frequency vs. temperature characteristics of the two thickness-shear modes of used SC quartz resonator simultaneously excited with assistance of the developed HT DMXO operating over extended temperature range between -45°C and +215°C.

VII. Conclusions

We have designed and evaluated HT DMXO with SC quartz resonator, which can operate without evidence of any activity dips over a wide temperature range, at least between -45°C and +215°C. The utilized higher 5th overtone fast thickness-shear mode, for which the resonant frequency almost linearly decreasing with temperature, is well suited for the SC resonator's self-thermometry implementation. Hence one can reduce frequency vs. temperature hysteresis, improve resolution, stability and accuracy in frequency control systems as well as in dual-mode piezoelectric pressure / temperature sensing systems requiring to operate in harsh high-temperature environment.

Acknowledgment

We would like to thank Zdenko Brezović, who helped to create useful MATLAB scripts for automatized derivation of equivalent resonator parameters from measured reflection scattering characteristics. Also, we would like to thank Jack A. Kusters from Agilent, and MtronPTI and Nofech Electronics Ltd. companies to provide us with samples of different SC quartz resonators.

References

[1] M. S. Patel and B. K. Sinha, "A dual-mode thickness-shear quartz pressure sensor for high pressure applications", IEEE Sensors J., vol. 18, no. 12, pp. 4893-4901, June 2018.

[2] M. S. Patel and B. K. Sinha, "Stress- and temperature-compensated orientations for thickness-shear langasite resonators for high-temperature and high-pressure environment", IEEE Trans. Ultrason. Ferroelectr. Freq. Control, vol. 62, no. 6, pp. 1095-1103, June 2015.

[3] I. Kocis, T. Kristofic, M. Gebura, G. Horvath, M. Gajdos and V. Stofanik, "Novel deep drilling technology based on electric plasma developed in Slovakia", Assembly and Scientific Symposium of the Union of Radio Science (URSI GASS), August 2017.

[4] V. Stofanik, P. Kubinec and E. Cocherova, "Dual-Mode Oscillator with SC Quartz Resonator Operating at Elevated Temperatures," Proc. of the 33rd International Conference RADIOELEKTRONIKA, Pardubice, Czech Republic, 2023, pp. 1-4.

[5] V. Stofanik, P. Kubinec, E. Cocherova and J. Pucik, " Design of Mode-Separation Filters for Dual-Mode Oscillator with SC Quartz Resonator Operating at Elevated Temperatures," Proc. of the 34th International Conference RADIOELEKTRONIKA, Zilina, Slovakia, 2024, pp. 1-4.

[6] E. P. EerNisse, "Quartz Resonator Frequency Shifts Arising from Electrode Stress", Proc. of the 29th Annual Symposium on Frequency Control, 1975, pp. 1-4.

[7] J. A. Kusters, "Transient Thermal Compensation for Quartz Resonators", IEEE Transactions on Sonics and Ultrasonics, Vol. SU-23, No. 4, July 1976, pp. 273-276.

[8] V. Stofanik, Z. Brezovic and M. Minarik, "Investigation of Drive Level Dependencies of Higher Overtones in SC Quartz Resonators", Proc. of the 2012 EFTF, Gothenburg, Sweden, 2012, pp. 227-234.

[9] V. Stofanik, Z. Brezovic, M. Minarik, E. Cocherova and P. Kubinec, "Investigation of amplitude effects on higher overtones in stress compensated quartz resonators," Proc. Of the 23rd International Conference RADIOELEKTRONIKA, Pardubice, Czech Republic, 2013, pp. 96-101.